Front. Optoelectron. China 2011, 4(1): 87–92
DOI 10.1007/s12200-011-0210-5

RESEARCH ARTICLE

Synthesis and photovoltaic property of pyrrole-based conjugated oligomer as organic dye for dye-sensitized solar cells

Qianqian LI[1], Wenjun WU[2], Aoshu ZHONG[1], Jianli HUA[2], Ming PENG[1], Jing HUANG[1], Jie SHI[1], He TIAN[2], Jingui QIN[1], Zhen LI (✉)[1]

1 Department of Chemistry, Wuhan University, Wuhan 430072, China
2 Key Laboratory for Advanced Materials and Institute of Fine Chemicals, East China University of Science & Technology, Shanghai 200237, China

Abstract A new pyrrole-based conjugated oligomer (P1) was obtained with phenyl-linked triphenylamine moieties as an isolation group. Little aggregations were observed whether oligomer P1 was absorbed on titanium dioxide (TiO_2) surface or in solid state. Since the pyrrole-based moieties in donor-π-acceptor type was the core component of oligomer P1 for light absorption, the corresponding dye-sensitized solar cell (DSSC) demonstrated the efficiency of light-to-electrical conversion by 0.48%. Higher conversion efficiency could be achieved by tuning the size of the isolation groups and the structure of the donor-π-acceptor type dyes.

Keywords pyrrole, synthesis, dye sensitizer, oligomer

1 Introduction

Dye sensitized solar cells (DSSCs) have attracted intense research interest due to their fabrication with low cost and high efficiencies of light-to-electrical conversion [1–5]. Although Ru-based complexes hold the efficiency recorded validated over 11% under full sunlight [6–9], their characteristics of high cost and relatively difficulty of purification limited their applications. On the other hand, organic dyes with easy structural tuning and generally high molar extinction coefficients have emerged as competitive alternatives to the Ru-based counterparts.

So far, many efficient organic dyes have been obtained, the highest efficiencies (η) of power conversion of DSSCs devices has achieved above 10% [10–14]. However, there were still some drawbacks to be overcome, such as the formation of aggregates on the surface of TiO_2 and the relatively fast charge recombination of the injected electrons in the film of TiO_2 with the redox species in the electrolyte. Thanks to enthusiastic efforts of chemists, some effective strategies have been proposed by extensive studies on molecular modification based on donor-π-acceptor configuration. Generally, the incorporation of the nonplanar structures into dye skeletons can hinder the π-π staking, and the introduction of long alkyl chains can block the redox species approaching the surface of TiO_2, decreasing the concentrations of redox species at the vicinity of the TiO_2, to increase the electron lifetime. Thus, our previous research has focused on the pyrrole-containing dyes [15,16], in which the triphenylamine (TPA) or indole was used as the electron donor, a cyanoacetic acid as the anchoring group. Another TPA group was introduced to the pyrrole ring through Carbon-Nitrogen single bond to suppress the possible aggregation of the dyes on the surface of TiO_2, or a carbazolyl group with alkyl chains was employed to decrease the charge recombination. All of these dyes exhibited good performance, and the highest conversion efficiency was as high as 7.21% (91% of the standard cell from N719, 7.88%, measured under the same conditions). Apart from these modifications of the dye structures, the property of the pyrrole ring played a very important role: as one of the strongest electron-rich five-member heterocyclics, its abundant electron density should be beneficial to the charge transfer from the donor to the acceptor [17].

Recently, Liu group reported that the incorporation of the donor-π-acceptor dyes into the conjugated polymers could be an effective method to enhance the conversion efficiency for polymer DSSCs [18]. For example, the conjugated polymer containing TPA as the electron donating backbone, and an electron accepting side chain

Received October 18, 2010; accepted December 30, 2010

E-mail: lizhen@whu.edu.cn

(cyanoacetic acid) with conjugated thiophene units as the linkers, gave good performance for the DSSC fabricated utilizing this material as the dye sensitizer. Thus, in view of the excellent properties of the pyrrole-based organic dyes, in this study, we designed a pyrrole-based conjugated oligomer, with phenyl-linked TPA as the isolation group, hexyloxyl and butyl moieties as the functional groups to align the oligomer and decrease the charge recombination. Here, the synthesis, structural characterization, electrochemical properties, and photovoltaic performance of pyrrole-based conjugated oligomer as organic dye for dye-sensitized solar cells were studied.

2 Experiment

2.1 Materials

Tetrahydrofuran (THF) was dried over and distilled from K-Na alloy under an atmosphere of dry argon. Compounds 1 and 2 were prepared following the procedure reported in the literatures [16,18]. All other reagents were used as received without further purification.

2.2 Instrumentation

^{1}H nuclear magnetic resonance (NMR) spectroscopy study was conducted with a Varian Mercury 300 spectrometer using tetramethylsilane (TMS; δ = 0 ppm) as internal standard. The Fourier transform infrared (FTIR) spectra were recorded on a Perkin Elmer-2 spectrometer in the region of 3000 – 400 cm^{-1} on NaCl pellets. Ultraviolet (UV)-visible spectra were obtained using a Schimadzu UV-2550 spectrometer. Gel permeation chromatography (GPC) analysis was performed on an Agilent 1100 series GPC system using a UV detector. Polystyrene standards were used as calibration standards for GPC. THF was used as an eluent and the flow rate was 1.0 mL/min. The electrochemical cyclic voltammetry was carried out on a CHI 600 voltammetric analyzer at room temperature in argon-purged anhydrous acetonitrile with tetrabutylammonium hexafluorophosphate (TBAPF$_6$) as the supporting electrolyte at a scanning rate of 100 mV/s. A platinum disk and an Ag/Ag$^+$ electrode were used as the working electrode and reference electrode, respectively. The ferrocene/ferrocenium redox couple was used for potential calibration.

2.3 Synthesis of oligomer P0

A mixture of compound 1 (1.00 g, 1.90 mmol), compound 2 (1.14 g, 1.90 mmol), sodium carbonate (2.01 g, 19.0 mmol), and tetrakis(triphenylphosphine)palladium (Pd (PPh$_3$)$_4$) (65.8 mg, 0.057 mmol) was carefully degassed and charged with argon. Subsequently, THF (60 mL) and deoxidized water (30 mL) were added by syringe. The reaction mixture was stirred at 80°C for 72 h. After cooled to room temperature, the organic layer was separated, THF was evaporated and methanol was added to precipitate the product, the oligomer P0 was further purified by reprecipitation with acetone/MeOH to afford yellow green solid P0 (0.78 g, 57.7%). M_w = 6700, M_w/M_n = 1.58 (GPC, polystyrene calibration). IR (thin film), υ (cm^{-1}): 1657 (-CHO). ^{1}H NMR (CDCl$_3$) δ (ppm): 10.04 and 9.33 (-CHO), 7.78 – 6.74 (ArH and –CH = CH-), 4.00 (-O-CH$_2$-), 3.81 (-*N*-CH$_2$-), 1.71 (-CH$_2$-), 1.28 (-CH$_2$-), 0.87 (-CH$_3$).

2.4 Synthesis of oligomer P1

The oligomer P0 (100 mg, 0.14 mmol) and cyanoacetic acid (16.2 mg, 0.19 mmol) were dissolved in THF (4 mL), and then 10 μL piperidine was added as the catalyst. The mixture was refluxed for 12 h. After cooled to room temperature, methanol was added to precipitate the product, the oligomer P1 was further purified by reprecipitation with acetone/MeOH to afford red solid P1 (70.5 mg, 60.7%). M_w = 3400, M_w/M_n = 1.55 (GPC, polystyrene calibration). IR (thin film), υ (cm^{-1}): 2214 (-CN). ^{1}H NMR (CDCl$_3$) δ (ppm): 7.98–6.24 (ArH and –CH = CH-), 4.21 – 3.64 (-O-CH$_2$- and-*N*-CH$_2$-), 2.08 (-O-CH$_2$-), 1.71 (-CH$_2$-), 1.26 (-CH$_2$-), 0.88 (-CH$_3$).

2.5 Photoelectrode preparation

A screen-printed double layer of TiO$_2$ particles was used as photoelectrodes. A 10 μm thick film of 13 nm size TiO$_2$ particles (Ti-Nanoxide T/SP) was first printed on the fluorine-doped tin oxide (FTO) conducting glass and further coated by a 4 μm thick second layer of 400 nm light scattering anatase particles (Ti-Nanoxide 300). Sintering was carried out at 450°C for 30 min. Before immersed in the dye solution, these films were soaked in 0.2 M aqueous titanium(IV) chloride (TiCl$_4$) solution overnight in a closed chamber, which has been proved to increase short-circuit photocurrent significantly. After being washed with deionized water and fully rinsed with ethanol, the films were heated again at 450°C for 30 min followed by cooling to 80°C and dipped into a 3×10^{-4} M solution of dyes in tetrahydrofuran (THF)/ethanol (2:3) for 12 h at room temperature.

2.6 Counter platinum (Pt)-electrodes preparation

The Pt electrode was deposited on the cleaned FTO glass by coating with a drop of platinum (VI) tetrachloride dihydride (H$_2$PtCl$_6$) solution (0.02 M in 2-Propanol solution) with heat treatment at 400°C for 15 min. A hole (0.8 mm diameter) was drilled in the FTO glass by a Drill-press as a counter electrode The perforated sheet was cleaned by ultrasound in an ethanol bath for 10 min.

2.7 DSSCs assemblage

The dye-covered TiO_2 electrode and Pt-counter electrode were assembled into a sandwich-type cell and sealed with a hot-melt gasket of 25 μm thickness made of the ionomer Surlyn 1702 (Dupont). The size of the TiO_2 electrodes used was 0.25 cm^2 (i.e., 5 mm × 5 mm). A drop of the electrolyte was put on the hole at the back of the counter electrode. It was introduced into the cell via vacuum back filling. The hole in the counter electrode was sealed by a film of Surlyn 1702 and a cover glass (0.1 mm thickness) using a hot iron bar.

2.8 Photoelectrochemical measurements

Photovoltaic measurements were employed by an AM1.5 solar simulator equipped with a 300 W xenon lamp (Model No. 91160, Oriel). The power of the simulated light was calibrated to 100 mW/cm^2 using a Newport Oriel PV reference cell system (Model 91150V). I (current)–V (voltage) curves were obtained by applying an external bias to the cell and measuring the generated photocurrent with a Keithley model 2400 digital source meter. The voltage step and delay time of photocurrent were 10 mV and 40 ms, respectively. Cell active area tested with a mask of 0.158 cm^2.

3 Results and discussion

3.1 Synthesis and characterization

The synthetic route was shown in Scheme 1. The oligomer P0 was obtained by the palladium-catalyzed *Suzuki* coupling reaction between compounds 1 and 2. Through the post-function of the oligomer P0 by Knoevenagel condensation reaction, oligomer P1 was prepared with high yield, as determined by the infrared (IR) spectra (Fig. 1). In the IR spectra of oligomer P1, the strong peak of the aldehyde group in the oligomer P0 at about 1660 cm^{-1} diminished, and the characteristic peak of the cyano (CN) group appeared at 2214 cm^{-1}. It should be pointed out that, by utilizing the *Suzuki* coupling reaction, different aryl moieties as the isolation group could be introduced into this system conveniently through single bonds. Thus, the size of steric hindrance for passivating the core component of the oligomer in donor-π-acceptor type could be tuned to optimize the properties of this material. Oligomer P1 was soluble in common solvents, such as THF, chloroform, dimethylfomamide (DMF)and dimethyl sulphoxide (DMSO). The molecular weight of oligomer P1 was determined by gel permeation chromatography (GPC) with THF as eluent, and polystyrene standards as calibration standards.

3.2 Optical properties

The UV-vis spectra of oligomer P1 were demonstrated in Fig. 2, while the maximum absorption wavelength ($\lambda_{\max}$) of the oligomer P1 in THF and on TiO_2 surface shown in Table 1. There were two distinct absorptions around 340 nm and 460 nm in the UV-vis spectra of oligomer P1. The absorption band around 340 nm was assigned to a π-π* transition, while the absorption band with $\lambda_{\max}$ around 460 nm corresponding to an intramolecular charge transfer (ICT) from the indole donor part to the acceptor end group. Compared to the UV-vis spectra of oligomer P1 tested in THF solution and in film, their $\lambda_{\max}$s were almost the same, indicating that there were nearly no aggregation in the solid state of oligomer P1. When the oligomer P1 was adsorbed on TiO_2 surface, the $\lambda_{\max}$ did not show a big difference in comparison with that tested in THF solution either, suggesting that most of the dyes adsorbed on TiO_2 surface were in the monomeric state. Its regular alignment should be ascribed to the rigid group, which was linked to the pyrrole moieties as the isolation group and its unique configuration.

3.3 Electrochemical properties

Cyclic voltametry was employed to investigate the redox behavior of oligomer P1 (Fig. 3). In the anodic scan, the onsets of oxidation of the oligomer P1 was found to occur at 0.69 V, which was converted to the normal hydrogen electrode (NHE) reference scale as 0.89 V, while the reduction potential *vs* NHE (E_{red}) could be calculated from E_{ox}-$E_{\text{o}-\text{o}}$ (Table 1). Both of the E_{ox} and E_{red} corresponded to the highest occupied molecular orbital (HOMO) and the lowest unoccupied molecular obtital (LUMO), respectively. As shown in Fig. 4, both LUMO and HOMO levels

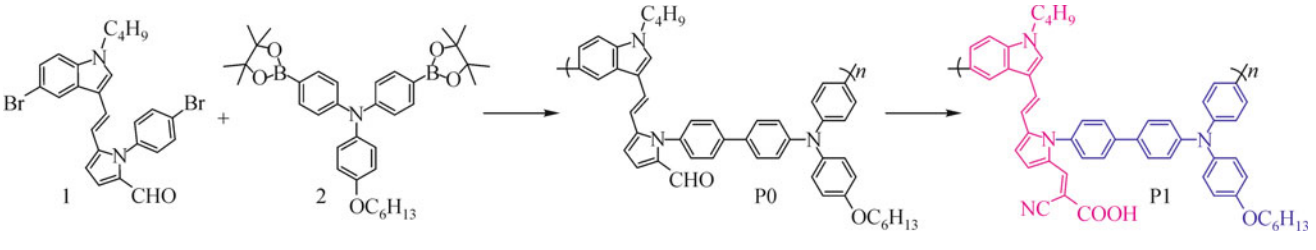

Scheme 1

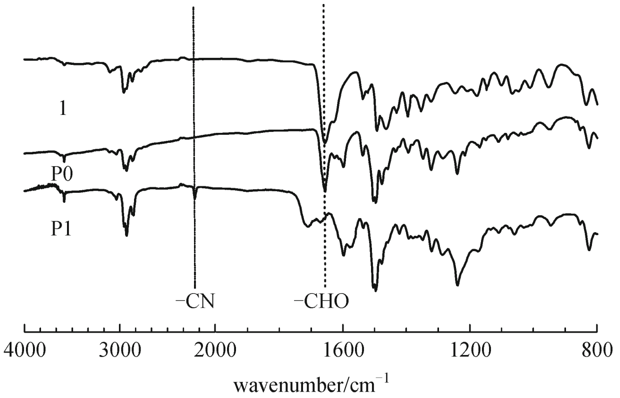

Fig. 1 IR spectra of monomer 1, oligomer P0 and P1

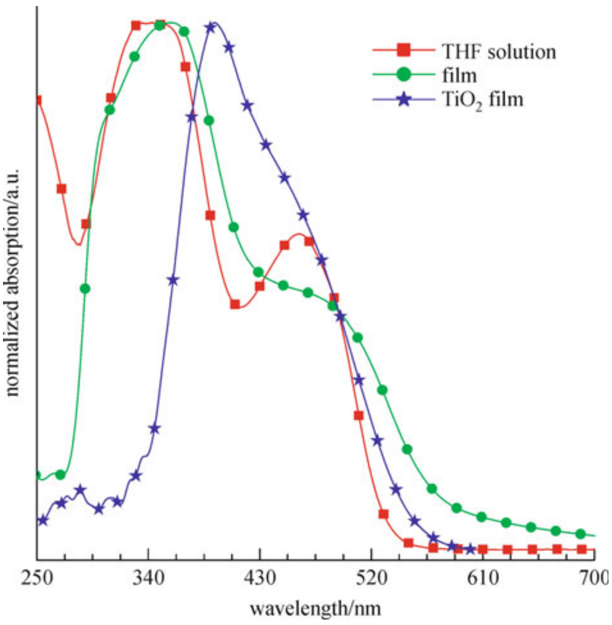

Fig. 2 UV-vis spectra of oligomer P1

of oligomer P1 agreed well with the requirements for an efficient dye sensitizer: first, the LUMO level was negative of the CB level (-0.5 V vs NHE) of TiO_2, and the E_{gap} was 0.77, indicating that the driving force was large enough for the injection; secondly, HOMO level of the oligomer P1 was more positive than the iodine redox potential (0.4 V), which ensured that the oxidized dye could be regenerated from the reduced species in the electrolyte.

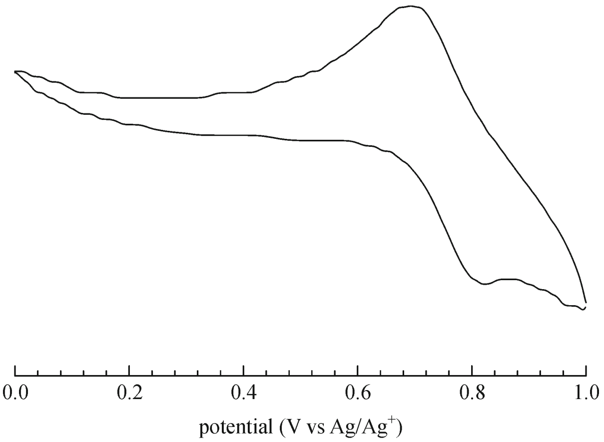

Fig. 3 Cyclic voltammograms of P1 films on platinum electrode in 0.1 mol/L Bu_4NPF_6, CH_3CN solution with a scan rate of 100 mV/s

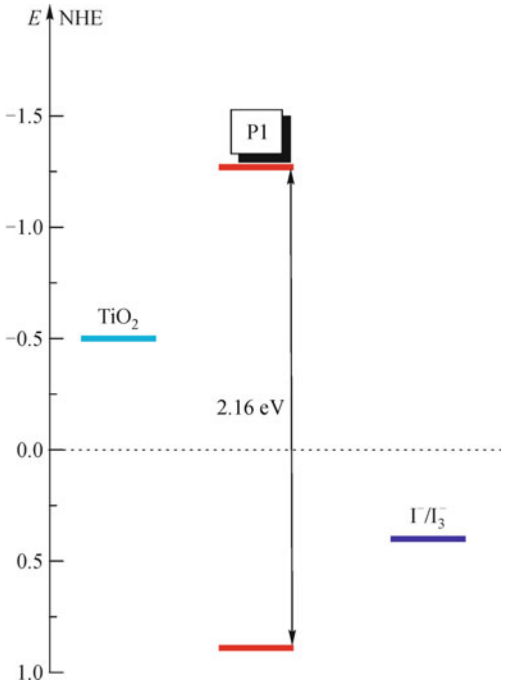

Fig. 4 Schematic representation of the band positions in DSSCs based on oligomer P1. Energy scale is indicated in electron volts using the normal hydrogen electrode (NHE)

Table 1 Some characterization data of P1

dye	M_w a)	M_w/M_n a)	λ_{max}/nm b)	ε at λ_{max} /($M^{-1}\cdot cm^{-1}$) b)	λ_{max}/nm c)	E_{0-0}/eV d)	E_{ox}/V e) vs NHE	E_{red}/V e) vs NHE	E_{gap}/V f)
LI-1	3400	1.5	462	21800	465	2.16	0.89	-1.27	0.77

Notes: a) Determined by GPC in THF on the basis of a polystyrene calibration. b) Absorption spectrum of oligomer P1 measured in THF with the concentration of 3×10^{-5} M. c) Absorption spectrum of oligomer P1 adsorbed on the surface of TiO_2. d) The bandgap, E_{0-0} was derived from the observed optical edge. e) The oxidation potential (E_{ox}) referenced to calibrated Ag/Ag$^+$ was converted to the NHE reference scale. E_{red} was calculated from E_{ox} - E_{0-0}. f) E_{gap} was the energy gap between the E_{red} of oligomer P1 and the CB level of TiO_2 ($-$ 0.5 V vs NHE)

3.4 Photovoltaic performance of DSSCs

Photovoltaic properties of the solar cell fabricated with the oligomer P1 was measured under simulated AM 1.5G irradiation. As shown in Fig. 5, the DSSC based on oligomer P1 gave a short-circuit photocurrent density (J_{sc}) of 1.22 mA/cm^2, an open-circuit voltage (V_{oc}) of 0.54 V, and a fill factor (*FF*) of 0.73, corresponding to an overall conversion efficiency (η) of 0.48%, without any of the additives typically used (e.g. 3a,4a-dihydroxy-5b-cholic acid) for enhancing conversion efficiencies. The relatively lower η value should be ascribed to the weak light harvesting capability of oligomer P1 on the surface of TiO_2. As seen from its absorption spectrum the surface of TiO_2, the alignment of the dyes was good, thus, the weak light harvesting capability should possibly be caused by the small amount of the dyes on TiO_2 surface, which was usually affected by the size of the isolation group and the configuration of the oligomer. For the core structure of oligomer P1 in donor-π-acceptor type, phenyl-linked TPA as the isolation group perhaps was too large. Although they could well suppress the possible aggregation, its large size decreased the effective component on the surface of TiO_2 for the light adsorption, then leading to the weak light harvesting capability. Therefore, in our further study, the size of the isolation group of the oilgomer should be adjusted to balance the two effects, the suppressing of the aggregations and the effective component on TiO_2 surface for absorbing light.

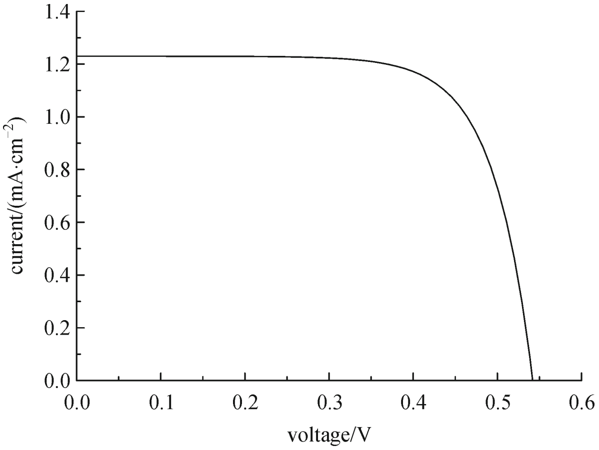

Fig. 5 Current density-voltage characteristics obtained with a nanocrystalline TiO_2 film supported on FTO conducting glass and derivatized with monolayer of the oligomer P1

4 Conclusions

In summary, we have demonstrated a new conjugated oligomer dye as an efficient organic sensitizer in DSSCs. After the incorporation of the donor-π-acceptor type dyes based on pyrrole as the core component and phenyl-linked TPA as the isolation group, the DSSC based on oligomer P1 gave a conversion efficiency of 0.48%. It was expected that higher conversion efficiencies of this kind of oligomers would be achieved by tuning the size of the isolation groups and the structure of the donor-π-acceptor type dyes.

Acknowledgements This work was supported by the National Natural Science Foundation of China (Grant No. 21002075) and China Postdoctoral Science Foundation (No. 20090460979).

References

1. Imahori H, Umeyama T, Ito S. Large π-aromatic molecules as potential sensitizers for highly efficient dye-sensitized solar cells. Accounts of Chemical Research, 2009, 42(11): 1809–1818
2. Grätzel M. Recent advances in sensitized mesoscopic solar cells. Accounts of Chemical Research, 2009, 42(11): 1788–1798
3. Preat J, Jacquemin D, Perpète E A. Towards new efficient dye-sensitised solar cells. Energy & Environmental Science, 2010, 3(7): 891–904
4. Ning Z, Fu Y, Tian H. Improvement of dye-sensitized solar cells: what we know and what we need to know. Energy & Environmental Science, 2010, 3(9): 1170–1181
5. Hagfeldt A, Boschloo G, Sun L, Kloo L, Pettersson H. Dye-sensitized solar cells. Chemical Reviews, 2010, 110(11): 6595–6663
6. Altobello S, Argazzi R, Caramori S, Contado C, Da Fré S, Rubino P, Choné C, Larramona G, Bignozzi C A. Sensitization of nanocrystalline TiO_2 with black absorbers based on Os and Ru polypyridine complexes. Journal of the American Chemical Society, 2005, 127 (44): 15342–15343
7. Wang P, Klein C, Humphry-Baker R, Zakeeruddin S M, Grätzel M. A high molar extinction coefficient sensitizer for stable dye-sensitized solar cells. Journal of the American Chemical Society, 2005, 127(3): 808–809
8. Gao F, Wang Y, Shi D, Zhang J, Wang M, Jing X, Humphry-Baker R, Wang P, Zakeeruddin S M, Grätzel M. Enhance the optical absorptivity of nanocrystalline TiO_2 film with high molar extinction coefficient ruthenium sensitizers for high performance dye-sensitized solar cells. Journal of the American Chemical Society, 2008, 130(32): 10720–10728
9. Bessho T, Yoneda E, Yum J H, Guglielmi M, Tavernelli I, Imai H, Rothlisberger U, Nazeeruddin M K, Grätzel M. New paradigm in molecular engineering of sensitizers for solar cell applications. Journal of the American Chemical Society, 2009, 131(16): 5930–5934
10. Zeng W, Cao Y, Bai Y, Wang Y, Shi Y, Zhang M, Wang F, Pan C, Wang P. Efficient dye-sensitized solar cells with an organic photosensitizer featuring orderly conjugated ethylenedioxythiophene and dithienosilole blocks. Chemistry of Materials, 2010, 22 (5): 1915–1925
11. Qin H, Wenger S, Xu M, Gao F, Jing X, Wang P, Zakeeruddin S M, Grätzel M. An organic sensitizer with a fused dithienothiophene unit for efficient and stable dye-sensitized solar cells. Journal of the American Chemical Society, 2008, 130(29): 9202–9203

12. Horiuchi T, Miura H, Sumioka K, Uchida S. High efficiency of dye-sensitized solar cells based on metal-free indoline dyes. Journal of the American Chemical Society, 2004, 126(39): 12218–12219
13. Koumura N, Wang Z S, Mori S, Miyashita M, Suzuki E, Hara K. Alkyl-functionalized organic dyes for efficient molecular photovoltaics. Journal of the American Chemical Society, 2006, 128(44): 14256–14257
14. Snaith H J, Petrozza A, Ito S, Miura H, Grätzel M. Charge generation and photovoltaic operation of solid-state dye-sensitized solar cells incorporating a high extinction coefficient indolene-based sensitizer. Advanced Functional Materials, 2009, 19(11): 1810–1818
15. Li Q, Lu L, Zhong C, Huang J, Huang Q, Shi J, Jin X, Peng T, Qin J, Li Z. New pyrrole-based organic dyes for dye-sensitized solar cells: convenient syntheses and high efficiency. Chemistry-A European Journal, 2009, 15(38): 9664–9668
16. Li Q, Lu L, Zhong C, Shi J, Huang Q, Jin X, Peng T, Qin J, Li Z. New indole-based metal-free organic dyes for dye-sensitized solar cells. Journal of Physical Chemistry B, 2009, 113(44): 14588–14595
17. Li Q, Lu C, Zhu J, Fu E, Zhong C, Li S, Cui Y, Qin J, Li Z. Nonlinear optical chromophores with pyrrole moieties as the conjugated bridge: enhanced NLO effects and interesting optical behavior. Journal of Physical Chemistry B, 2008, 112(15): 4545–4551
18. Lim E, Kim M, Lee J, Jung B J, Cho N S, Lee J, Do L M, Shim H K. Relationship between the liquid crystallinity and field-effect-transistor behavior of fluorene-thiophene-based conjugated copolymers. Journal of Polymer Science A: Polymer Chemistry, 2006, 44 (16): 4709–4721